J Atmos Chem (2011) 68:27–53
DOI 10.1007/s10874-010-9177-7

Sources, transport, and sinks of SO_2 over the equatorial Pacific during the Pacific Atmospheric Sulfur Experiment

Burton Alonza Gray · Yuhang Wang · Dasa Gu · Alan Bandy · Lee Mauldin · Antony Clarke · Becky Alexander · Douglas D. Davis

Received: 8 August 2010 / Accepted: 3 November 2010 /
Published online: 19 November 2010

Abstract The Pacific Atmospheric Sulfur Experiment (PASE) is the first sulfur-budget field experiment to feature simultaneous flux measurements of DMS marine emissions and SO_2 deposition to the ocean surface. We make use of these data to constrain a 1-D chemical transport model to study the production and loss pathways for DMS and SO_2 over the equatorial Pacific. Model results suggest that OH is the main sink for DMS in the boundary layer (BL), and the average DMS-to-SO_2 conversion efficiency is ~73%. In an exploratory run involving the addition of 1 pptv of BrO as a second oxidant, a 14% increase in the DMS flux is needed beyond that based on OH oxidation alone. This BrO addition also reduces the DMS-to-SO_2 conversion efficiency from 73% to 60%. The possibility of non-DMS sources of marine sulfur influencing the estimated conversion efficiency was explored and found to be unconvincing. For BL conditions, SO_2 losses consist of 48% dry deposition, while transport loss to the BuL and aerosol scavenging each account for another 19%. The conversion of SO_2 to H_2SO_4 consumes the final 14%. In the BuL, cloud scavenging removes 85% of the SO_2, thus resulting in a decreasing vertical profile for SO_2. The average SO_2 dry deposition velocity from direct measurements (i.e., 0.36 $cm\,sec^{-1}$) is approximately 50% of what is calculated from the 1-D model and the global GEOS-Chem

B. A. Gray (✉) · Y. Wang · D. Gu · D. D. Davis
School of Earth and Atmospheric Sciences, Georgia Institute of Technology, Atlanta, GA 30332-0340, USA
e-mail: burton.gray@gatech.edu

A. Bandy
Chemistry Department, Drexel University, Philadelphia, PA 19104-2875, USA

L. Mauldin
Atmospheric Chemistry Division, National Center for Atmospheric Research, Boulder, CO 80307, USA

A. Clarke
School of Ocean and Earth Science and Technology, University of Hawaii, Manoa, Honolulu, HI 96822, USA

B. Alexander
Department of Atmospheric Sciences, University of Washington, Seattle, WA 98195-1640, USA

model. This suggests that the current generation of global models may be significantly overestimating SO_2 deposition rates over some tropical marine areas. Although the specific mechanism cannot be determined, speculation here is that the dry deposition anomalous results may point to the presence of a micro-surface chemical phenomenon involving partial saturation with either S(IV) and/or S(VI) DMS oxidation products. This could also appear as a pH drop in the ocean's surface microfilm layer in this region. Finally, we propose that the enhanced SO_2 level observed in the lower free troposphere versus that in the upper BuL during PASE is most likely the result of transported DMS/SO_2-rich free-tropospheric air parcels from the east of the PASE sampling area, rather than an inadequate representation in the model of local convection.

Keywords Sulfur field study · Airborne sampling · Chemical modeling · Dimethyl sulfide oxidation · Sulfur dioxide formation and losses · Dry deposition · Aerosol scavenging

1 Introduction

The marine biogenic compound dimethyl sulfide (DMS) is of considerable interest due to its defining the planet's largest natural sulfur source. It is, therefore, the single largest natural source of sulfur aerosols (Lovelock et al. 1972; Kritz 1982; Andreae and Raemdonck 1983; Andreae et al. 1995). Sulfur aerosols, in the form of cloud condensation nuclei (CCN), are pivotal to our understanding of both local and regional weather patterns. As such, they represent an important component in advanced modeling efforts designed to assess global climate trends (Ghan et al. 1990; Hegg et al. 1990; Thomas et al. 2010). This effort has received increasing attention since 1987 with the publication by Charlson et al. (1987) of a natural climate feedback system that assigned DMS as the pivotal chemical species. The proposed scheme has phytoplankton-generated DMS leading to the formation of CCN which, in turn, modulate solar radiation, and hence, phytoplankton populations. Though many of the scientific components making up this 1987 hypothesis were at the time poorly understood, research efforts over the last two decades have provided considerable enlightenment on a number of these. For example, laboratory studies have now revealed that several different chemical processes can lead to the atmospheric oxidation of DMS. One of those of central importance involves the atmospheric oxidant OH (hydroxyl radical). Interestingly, as first demonstrated by Hynes et al. (1986), the OH oxidation of DMS proceeds by two independent chemical pathways. The abstraction channel, having a positive activation energy, is heavily favored under tropical conditions; but even at elevated temperatures, the addition channel, with a negative temperature dependence, still contributes upwards of 20–25% to the oxidation process (e.g., valid over the range 23°–28°C).

These and still other laboratory kinetic studies (Barone et al. 1996; Urbanski et al. 1998; Williams et al. 2001; Kukui et al. 2003) have focused on quantifying the individual steps in the overall oxidation mechanism; whereas, field and laboratory chamber studies (Bandy et al. 1996; Davis et al. 1999; Arsene et al. 1999; Nowak et al. 2001; Arsene et al. 2002; Read et al. 2008a) have provided more detailed information on the reaction products resulting from the DMS oxidation process. Two of the more significant of these are SO_2 and methanesulfonic acid (MSA). SO_2, however, is itself quite reactive and, either by heterogeneous reactions or gas phase processes, typically converts to S(VI) within one to 2 days under boundary layer (BL) conditions. The product from the gas-phase reaction, H_2SO_4, is also removed from the atmosphere quickly but has been directly observed in several field studies (Davis et al. 1999; Mauldin et al. 1999; Weber et al. 2001). The

existing evidence suggests that SO_2 is the major product formed from the abstraction channel; whereas, the highly reactive sulfur species dimethyl sulfoxide (DMSO) appears to be the initial major product from addition.

Early field studies carried out at tropical latitudes, the primary focus of this paper, presented a conflicting picture regarding the chemical link between DMS and the product SO_2. One of the earliest efforts revealing a strong chemical linkage was that reported by Bandy et al. (1996). In this Christmas Island study, simultaneous measurements of DMS and SO_2 were continuously recorded during two 5-day sampling periods. DMS conversion to SO_2 was clearly evident in there being observed a strong anti-correlation between these two species. Yet in a still earlier ship-board tropical study, reported by Huebert et al. (1993), virtually no relationship was seen between these species, though the temporal resolution in this study was sufficiently low that it would have been difficult to see an anti-correlation. And, in another tropical study in the South Pacific, ship-board measurements reported by Yvon et al. (1996) showed only a modest anti-correlation between DMS and SO_2 (i.e., 40%). By comparison, the Bandy et al. Christmas Island study resulted in a DMS-to-SO_2 conversion efficiency of 62%. Chen et al. (2000), using the same data set, employed an updated DMS oxidation mechanism in which the optimum model-estimated conversion efficiency was quite similar, i.e., 65%. Finally, in an airborne study also carried out near Christmas Island, Davis et al. (1999), using simultaneous measurements of DMS, SO_2, MSA, H_2SO_4, and OH in conjunction with box-model calculations, estimated a DMS-to-SO_2 conversion rate of 72%. Interestingly, Faloona (2009) in his survey of the literature found that of nine global 3-D studies in which DMS emissions were included, the DMS-to-SO_2 conversion efficiency of the respective models was greater than or equal to 85%. The latter value, however, unlike the tropical studies cited above, was undoubtedly influenced by the inclusion of large-scale DMS oxidation in the free troposphere. In this setting, both the absence of aerosols and the presence of rather low temperatures favor the production of SO_2.

As cited above, although reaction with OH has long been viewed as the major pathway for oxidizing DMS, more recent laboratory and field studies suggest that even under pristine conditions halogen species might also be important (Barnes et al. 1991; Ingham et al. 1999; Dyke et al. 2006; Saiz-Lopez et al. 2007). In one such study, bromine oxide (BrO) was measured in the North Atlantic under tropical conditions (Read et al. 2008b) with reported values as high as 4 pptv and a mid-day average of ~2 pptv. Although such low concentrations might initially suggest the inefficiency of these species, rate constant data suggests that even at mixing ratios as low as 1 pptv, BrO has the potential to compete with OH as a primary DMS oxidant.

Further complicating the assessment of the impact of DMS emissions on the sulfur budget is the array of loss mechanisms by which SO_2 can be removed within the marine BL. In addition to the previously mentioned reaction with OH, both deposition to the ocean's surface as well as scavenging by local aerosols can form effective sinks for this species. Quite relevant to the current study, none of the previously listed field work has been able to clearly establish the relative importance of these removal processes, due in large part to the absence of an independent method for measuring SO_2 deposition to the surface (Faloona 2009).

Although under tropical BL conditions CN (condensation nuclei) formation (e.g., from the production of H_2SO_4) is typically considered unlikely, Clarke et al. (1998) convincingly showed that even here bursts of CN particles can form in the absence of marine aerosols, e.g., under conditions reflecting the impact of a major rain event. The latter occurrence then points to one of the critical pieces of information required to fully assess the impact of DMS on CN

production, namely, the efficiency with which this species is transported from the BL to an environment having a low aerosol loading. This is typically found in the atmospheric marine regions identified as the buffer layer (BuL) (Russell et al. 1998) and the lower free troposphere (FT). As will be discussed later in the text, in the current study we have used a 1-D chemistry and transport model to assess the efficiency of this process.

Of the many uncertainties remaining in defining the role of DMS emissions in the formation of tropospheric CN, among the larger of these is the ocean-to-atmosphere flux. For example, from an examination of the five most recent global-study publications reported in the Faloona (2009) paper (i.e., Liu et al. 2007; Verma et al. 2007; Koch et al. 2006; Kloster et al. 2006; Berglen et al. 2004), estimates of the global DMS flux ranged from 12 to 28 Tg S per year. Still other uncertainties influencing the atmospheric marine sulfur budget in the tropical Pacific include: The efficiency with which DMS is converted to SO_2 and how the magnitude of this quantity may vary as a function of local chemical composition; the influence of halogens and possibly unknown additional sulfur sources; the relative impact of various chemical and physical processes on SO_2 removal; and the impact of long-range transport of sulfur relative to that locally generated.

The Pacific Atmospheric Sulfur Experiment (PASE) has provided two major advantages over previous field experiments in its efforts to evaluate critical aspects of the marine sulfur budget: 1) the DMS ocean flux is directly measured, thus constraining the largest source of reduced sulfur to the atmosphere, and (2) the SO_2 deposition flux to the ocean is also directly measured, thereby constraining one of the major sinks for this DMS oxidation product. The overarching objective of this work is that of providing further insight into the role of DMS emissions in influencing the formation of CN particles under tropical-tropospheric conditions. Reflecting the uncertainties cited above, the approach taken here will use a 1-D chemistry and transport model to evaluate the following specific objectives: a) the chemical efficiency with which DMS is converted to the product species SO_2; b) the contribution that non-OH (i.e., halogen species) oxidants might make in oxidizing DMS; c) the impact of BuL clouds on the vertical distribution of SO_2; d) the relative contributions made by dry deposition, aerosol scavenging, and vertical transport on BL SO_2 levels; and (e) the relative importance of local sulfur sources versus long-range transport in controlling sulfur levels in the lower free troposphere.

2 Observations

2.1 PASE aircraft data

Fourteen research flights were conducted during the PASE mission using the National Center for Atmospheric Research (NCAR) C-130 H. Flights were based out of Christmas Island (2ºN, 157ºW) and took place between August 8 and September 6 of 2007. All of the research flights were conducted over the area of 1ºS–4ºN and 153º–159ºW, with the exception of flight 4, which was flown further north as a cloud sampling mission. All of the research flights were in excess of 8 h duration, except for flight 7, which was shortened to just a few hours due to difficulty in procuring aircraft fuel. The aircraft flight patterns are discussed in detail by Conley et al. (2009) and Faloona et al. (2010).

For this study, flights 2, 3, 5, 8, 11, and 12 are used for a daytime comparison to the model results. The data from flight 1 were not used due to a lack of DMS measurements. Flights 4 and 7 were eliminated for the reasons discussed in the above paragraph. Flights 9 and 10 were not included due to errors resulting from problems with the aircraft's inertial

navigation system. This did not allow for an appropriate measurement of wind speed, resulting in our inability to define either the BL or BuL heights for those two flights. Finally, data from flight 14 were removed because the daytime average DMS concentration was 50% higher than the average from the other six flights chosen for this analysis (Conley et al. 2009).

Although potentially providing considerable insight regarding the loss of SO_2 to aerosols and to dry deposition, nighttime flights 6 and 13 were also excluded from the final database used in this study. This decision was based on the fact that the observations from these two flights showed a great deal of inconsistency. As an important example, flight 6 had average pre-dawn concentrations of DMS and SO_2 of 87 and 27 pptv, respectively; whereas, flight 13 generated average values of 113 and 28 pptv, respectively. In addition, there were significant differences seen in the latitudinal gradient for SO_2. During flight 6, it was >10 pptv deg^{-1}; for flight 13, it was less than 3 pptv deg^{-1}. Thus, given that these were the only two nighttime flights producing data, we chose to restrict the current analysis to the more consistent daytime flights 2, 3, 5, 8, 11, and 12.

Several PASE aircraft measurements served as primary constraints for carrying out the modeling analyses presented in the text that follows. Pivotal were the measured values for BL DMS and OH. Techniques employed to measure the most critical species during the PASE study covered a wide range of instrumentation. DMS and SO_2 were measured using atmospheric-pressure ionization mass spectrometers (APIMS) (Bandy et al. 2002; Thornton et al. 2002; Huebert et al. 2004; Blomquist et al. 2006). The two vertical fluxes that were directly measured used eddy covariance methodology (Fairall et al. 2000). Liquid water content (LWC) measurements were made using a Gerber PV-100 probe. This probe was also used to determine the presence or absence of clouds in the BuL. LWC measurements of >0.01 gm^{-3} were taken as the basis for the presence of clouds. OH measurements utilized the technique selected-ion chemical-ionization mass spectrometry (SICIMS) (Mauldin et al. 1998). Ozone observations were recorded using a fast chemiluminescence instrument (Ridley et al. 1992). Finally, aerosol size and distribution measurements covering the range of 0.01 to 10 μm were carried out using several different instruments, as previously described by Clarke et al. (2004).

2.2 CH_3I aircraft data

Measurements of the short-lived species methyl iodide (CH_3I) have been used to constrain our 1-D model for purposes of assessing vertical transport over tropical regions, e.g., Wang et al. (2000, 2001). Given, however, that no measurements of this species were recorded during this study, CH_3I observational data recorded during NASA's PEM-Tropics A and B field studies were used. Both studies involved field operations in the equatorial Pacific, Christmas Island being a major base of operation. With a lifetime of ~6 days, these CH_3I data revealed that during PEM-Tropics A (1997), levels were reasonably consistent with dry season conditions; whereas, during PEM-Tropics B (1999), the profile resembled those of the wet season.

2.3 Satellite and other data

Sea surface temperature (SST) was used as an indicator of upwelling regions in the equatorial Pacific as these regions tend to be colder than their surroundings. Since these cold regions typically reflect areas of elevated nutrients, enhancements in phytoplankton and bacterial populations are common. Although the latter can frequently lead to major

increases in DMS, this conclusion is much dependent on phytoplankton types. We have used SST data from the National Oceanic and Atmospheric Administration (NOAA) Environmental Modeling Center to identify these likely upwelling regions. The NOAA SST data are a combination of in-situ and satellite data and are released as weekly- and monthly-averaged fields.

Measurements of chlorophyll concentration are one of the methods employed to assess sea-surface biogenic activity, though chlorophyll and DMS concentrations do not always strongly correlate (Kettle et al. 1999). In this study, data from the NASA National Earth Observatory (NEO) were used to determine sea-surface chlorophyll concentrations, thus identifying potential areas having DMS enhancements. The data were obtained via the Moderate-resolution Imaging Spectroradiometer (MODIS) instrument onboard the Aqua satellite.

In addition to identifying marine areas with potentially enhanced DMS, satellite imagery was also used to examine cloud top temperatures. These data provided one estimate of convection in and around the PASE sampling area. The source of this data was again the MODIS instrument aboard the Aqua satellite.

3 Model descriptions

3.1 REAM model

3.1.1 General characteristics

The Regional chEmical trAnsport Model (REAM) used in this study is a 1-D version of the 3-D REAM model described by Zhao et al. (2009a). Previously, this model has been used to study tropospheric chemistry and transport in North America (Zhao et al. 2009a; Choi et al. 2005, 2008a, b; Wang et al. 2006), Southeast Asia (Zhao and Wang 2009; Zhao et al. 2009b, 2010), the Arctic (Zeng et al. 2003, 2006), and the Antarctic (Wang et al. 2008). This version of REAM uses meteorological fields from the Weather Research and Forecasting (WRF) model (Skamarock et al. 2005).

The meteorological fields were assimilated using the WRF model on the basis of the National Center for Environmental Prediction (NCEP) reanalysis fields. The WRF model has a horizontal resolution of 10 km with 45 vertical layers below 10 hPa. Meteorological fields in the 1-D REAM model are updated every half hour, except for those related to convection, which are updated every 5 min. For each flight, 1-D meteorological parameters along the entire flight track were used. Hourly averages over the sampling region were taken for times outside the flight period. Diurnal simulations were run for 30 consecutive days using the same meteorological fields as defined on a specific flight day to obtain quasi-steady-state 1-D results. Sensitivity tests indicate that extending the run time out to 60 days returned basically the same results. Carbon monoxide (CO), O_3, and water vapor were constrained according to PASE observations for each flight, as were BL OH levels. The NO_x mixing ratio was fixed at 2 pptv, consistent with previous measurements in this region (Wang et al. 2001).

3.1.2 Turbulent diffusion in the buffer layer

The WRF model is unable to reproduce the intermittent turbulence typical of the BuL. It instead yields a sudden transition between a fully turbulent BL and the more stable FT.

Thus, in the 1-D REAM model, BL and BuL heights were set according to PASE observations; however, the BuL turbulent diffusion coefficient is specified from the CH_3I profiles generated from the PEM-Tropics A and B studies (see above discussion).

3.1.3 Sulfur module

A sulfur module was added to the standard version of REAM. The modeled species are DMS, SO_2, dimethyl sulfoxide (DMSO), methane sulfinic acid (MSIA), methane sulfonic acid (MSA), and sulfuric acid (H_2SO_4). Since this study has as its major focus DMS and SO_2, the final oxidation products MSA and H_2SO_4 had little impact on our results. The addition channel products DMSO and MSIA, on the other hand, represent intermediates that play a critical role in defining the conversion efficiency of DMS to SO_2 since under BL conditions they are predominantly scavenged by aerosols, leading to the production of methane sulfonate (MS).

Ocean flux Marine DMS emissions are known to be the major source of SO_2. Thus, in this study, DMS was the only sulfur emission species directly measured. In running the REAM model, DMS concentrations were adjusted in the first layer according to a diurnally-varying boundary condition. The latter was constructed using PASE observational data as defined by the subset of PASE flights used in this study, as cited earlier in the text. This was done by first creating an hourly median using the observational data, and then adjusting the REAM DMS concentration in the first layer to match the BL observations. The DMS ocean flux was inferred from the model through a budget analysis.

Gas-phase chemistry The chemical module was that reported by Chen et al. (2000). Rate constants and branching ratios for the gas-phase reactions were updated from Zhu et al. (2006) and are shown in Table 1. DMS in the model was given no chemical source and was oxidized by OH, BrO, or both depending on the science question being addressed. In the current gas-phase chemical modeling scheme, DMSO and MSIA are the major products resulting from the DMS addition channel. In this scheme, DMSO either reacts with OH or is scavenged by aerosols. When reacting with OH, it produces MSIA, which can either further react with OH or again be scavenged by aerosols. Upon reaction with OH, it

Table 1 Gas-phase sulfur reactions and rate constants[a,b]

Reaction	k(T), cm^3 $molec^{-1}$ s^{-1}
[c]DMS + OH → $0.9SO_2$ + $0.1H_2SO_4$ (Abstraction)	[d]$1.10\times10^{-11}\exp(-240/T)$
DMS + OH → 0.5DMSO + $0.2DMSO_2$ + 0.3MSIA (Addition)	$(1.0\times10^{-39}\exp(5820/T)[O_2])$ $(1+5.0\times10^{-30}\exp(6280/T)[O_2])$
DMSO + OH → $0.9MSIA + 0.1DMSO_2$	9.0×10^{-11}
MSIA + OH → $0.9SO_2$ + 0.1MSA	9.0×10^{-11}
SO_2 + OH → H_2SO_4	[e]$k_{12}=F \times k_0 \times k_\infty/(k_0+k_\infty)$

[a] Reproduced from Zhu et al. (2006).

[b] For heterogeneous scavenging processes (e.g., DMSO and MSIA), please see section 3.1.3.

[c] We assume 100% conversion of $CH_3SCH_2O_2$ to SO_2 or H_2SO_4.

[d] Newer value from Sander et al. (2006).

[e] $\log F=\log(0.525)/(1+[\log(k_0/k_\infty)]^2)$, $k_0=4.5\times10^{-31}(T/300)^{-3.9}$ [M], $k_\infty=1.26\times10^{-12}(T/300)^{-0.7}$

predominately yields SO_2. SO_2 is also the major product resulting from the OH/DMS abstraction channel even though, as discussed later in the text, it is quite possible that the sulfur intermediate (CH_3SCH_2OOH) from the abstraction channel could potentially be lost to aerosol scavenging. The only gas-phase reaction considered for SO_2 was that with OH, but as noted above for several other sulfur species, aerosol scavenging was also included as a sink mechanism.

Dry deposition The SO_2 deposition velocity was either fixed according to PASE observations (Faloona et al. 2010) or calculated using the resistance-in-series scheme of Wesely (1989), a scheme also used in the GEOS-Chem model (Wang et al. 1998). For DMSO and MSIA, the deposition velocities were calculated.

Cloud scavenging During the PASE study, clouds appeared in the BuL only. As such, cloud scavenging in the REAM model was limited to this region. The scavenging rates for all soluble sulfur species (SO_2, DMSO, MSIA) were assigned the same value. Based on LWC data from the Gerber PV-100 probe, clouds were typically present in only 2–3% of the BuL flight-track data points. Under these conditions we have estimated that the lifetime for a soluble species in the BuL would best be given by the time it took a species to fully mix within the cloud-free portion of the BuL. It was further assumed that a soluble species would be scavenged immediately upon cloud contact. For this scenario, the lifetime is given by:

$$\tau = \frac{L^2}{2K_z} \tag{1}$$

where τ is the BuL mixing time, K_z is the BuL turbulent diffusion coefficient, and L is the BuL thickness, minus the cloud coverage percentage. This parameterization is relatively insensitive to cloud volume when the latter is low. For instance, if one assumes that 2% of the BuL volume is in clouds (where clouds are defined as LWC>0.01 gm^{-3}), then a five-fold increase in cloud volume (i.e., an additional 8% reduction in L) would decrease SO_2 residency time in the BuL by only 16%.

Aerosol scavenging Because of its low solubility (particularly at high temperatures) and low reactivity, DMS removal by aerosols and its subsequent reaction with O_3 was assigned a negligible rate (Gershenzon et al. 2001; Lee and Zhou 1994). DMSO and MSIA, on the other hand, are very soluble, and their aerosol scavenging rates were estimated via the following formula:

$$k = D_g \int \left(\frac{2F(Kn,\alpha)}{D_p} \frac{dA}{d\log D_p} \right) d\log D_p \tag{2}$$

Here k is the scavenging rate in sec^{-1}, D_g is the gas diffusivity in air, A is the aerosol surface area concentration, D_p is the aerosol particle diameter, and F is the transition regime formula for the diffusion of a gas species from air to an aerosol. F is a function of Knudsen number (Kn) and sticking coefficient (α), and is determined according to the Dahneke formulation by Seinfeld and Pandis (1998).

In the case of SO_2, its uptake is driven by its ability to react with O_3 in the aqueous phase. However, since its rate slows with decreasing pH, the uptake to aerosols is limited by the available alkalinity (Chameides and Stelson 1992). In other words, surface uptake of

SO_2 using Eq. (2) is higher than the supply of available alkalinity (for other aerosol chemical losses of SO_2, please see discussion later in this text). Our model calculation shows that this is indeed the case during the PASE experiment. As a result, most SO_2 aerosol loss is confined to the coarse-mode size range of sea salt. In estimating this species loss, therefore, it was first necessary to calculate the alkalinity flux from the ocean in the form of emitted aerosols, i.e.,

$$F_{Alk} = \rho_{ss} Alk_{ss} \int \left(v_d \frac{dV}{d \log D_p} \right) d \log D_p \tag{3}$$

where F_{Alk} is the alkalinity flux in $\mathrm{eq\,m^{-2}\,s^{-1}}$, ρ_{ss} is the sea-salt aerosol density, Alk_{ss} is the aerosol alkalinity, v_d is the size-dependent aerosol deposition velocity, V is the aerosol volume concentration, and D_p is the aerosol particle diameter. This approach is adapted from Chameides and Stelson (1992). In this formulation, the deposition velocity of sea salts is determined according to Slinn and Slinn (1981). The sea-salt flux is assumed to be the same as the deposition flux (Smith et al. 1993). Sea-salt aerosols are also assumed to have the same composition as seawater. Given an average seawater alkalinity of 0.0025 eq/kg, this converts to a dry sea-salt equivalent of 0.07 eq/kg (Gurciullo et al. 1999). One mole of SO_2 consumes two alkalinity equivalents. In the above calculation, the aerosol size data employed was that based on direct measurements during the PASE study.

In an earlier method used to estimate the aerosol flux, the assumption was made that a balance is always reached between the aerosol flux entering the ocean and that leaving (Smith et al. 1993). According to Petelski (2003), however, this is rarely achieved. Clarke et al. (2006), on the other hand, have determined that the aerosol flux rate is typically much larger than that calculated using the Smith et al. approach. Here both options have been considered, as discussed in section 4, with the Smith et al. approach being used in our standard REAM model.

Because of the much lower loading of large aerosols in the BuL, SO_2 uptake by aerosols was confined to only the BL. For much smaller aerosols, we have assumed that by the time these particles reach the BuL, their alkalinity will have been consumed by absorption of various acidic compounds, leaving them ineffective as a removal pathway for SO_2.

However, as noted above, some SO_2 may also be lost to aerosol scavenging via its aqueous reaction with H_2O_2. Under PASE BL conditions, though, we estimate this loss to be negligible. For example, taking a BL H_2O_2 concentration of 2 ppbv with an aerosol volumetric concentration of 50 $\mu m^3/cm^3$ (two to five times more than seen during PASE flights), we estimate an SO_2(g) loss rate of only 0.1% per hour in the BL due to its reaction with aerosol H_2O_2 using the method outlined by Seinfeld and Pandis (1998).

3.2 GEOS-chem global model

The model setup for GEOS-Chem has been described by Alexander et al. (2005). This model uses assimilated meteorological data from the NASA Goddard Earth Observing System (GEOS). GEOS meteorological fields have a horizontal resolution of 1° latitude by 1° longitude, with 30 vertical sigma levels. The horizontal resolution is degraded to 4° by 5° for input into GEOS-Chem. The sulfur module is as described by Park et al. (2004) with the exception of ship SO_2 emission data, as described by Corbett et al. (1999). DMS, SO_2, sulfate, and MSA are all included in the model. For SO_2, the gas-phase oxidation is via reaction with OH, and the in-cloud oxidation is controlled by reaction with hydrogen peroxide (H_2O_2) and O_3. Cloud water pH is calculated utilizing the ISORROPIA II aerosol

thermodynamic model (Fountoukis and Nenes 2007). Sea-salt aerosol emissions are calculated based on local wind speed and sea-surface temperature as described in Jaeglé et al. 2010.

SO_2 aerosol loss is driven by available alkalinity. If the total flux of H_2SO_4, SO_2, and nitric acid (HNO_3) to sea-salt aerosols is less than the local alkalinity flux, then the uptake of SO_2 by aerosols is calculated as the flux rate to aerosols. This rate is typically much slower than the aqueous reaction of S(IV) with O_3, thereby making it the rate-limiting step. However, if the local alkalinity flux does not exceed the combined total flux of acidic compounds to the sea-salt aerosols, the SO_2 loss rate is then decreased as it must compete with H_2SO_4 and HNO_3 for the available alkalinity.

3.3 HYSPLIT trajectory model

The NOAA HYbrid Single-Particle Lagrangian Integrated Trajectory (HYSPLIT) model has been used to compute back-trajectories for the PASE sampling region, as well as for surrounding areas outside this region. These back-trajectories were calculated directly on the NOAA HYSPLIT website (Draxler and Rolph 2010; Rolph 2010) using the GDAS (Global Data Assimilation System) meteorology data from NCEP.

4 Results and discussion

4.1 Standard REAM model results

In Fig. 1a, we show the raw data for DMS and SO_2 as a function of altitude. In Fig. 1b, box plots reflecting the inner quartiles of the raw sulfur data, as well as for CH_3I, are shown along with the median values generated from our standard model. As noted earlier, since CH_3I was not measured during PASE, we have used the DC-8 and P-3B measurements recorded during the PEM-Tropics A (9ºS to 7ºN) and PEM-Tropics B (11ºS to 2.5ºN) field studies. These data were filtered according to geographical coordinates so as to generally overlap the region defined by the PASE sampling flights. The PEM-Tropics methyl nitrate measurements (not shown) were also used to further confirm the uniformity of biogenic emissions across this region.

As shown in Fig. 1b, the CH_3I model results agree well with those from PEM-Tropics A and B up to ~1,250 m. The mean BL and BuL heights during PASE were 550 m and 1,300 m, respectively (the BL and BuL height ranges were 425–660 m and 1,130–1,385 m, respectively). In the model runs, WRF-simulated turbulent diffusion coefficients were used in the BL and lower FT; whereas, for the BuL, a K_z value was specified of 2 $m^2 s^{-1}$ in an effort to capture the CH_3I gradient. The large differences seen between the PEM-Tropics A and B profiles for the lower FT versus those predicted by the REAM model reflect the much weaker convection experienced during PASE than PEM-Tropics A and B (Dasa Gu, unpublished results). This is seen in the higher BuL heights observed in PEM-Tropics A (Davis et al. 1999) and PEM-Tropics B (Nowak et al. 2001), e.g., 1,500–1,800 m. A similar difference is also seen in the respective vertical profiles for relative humidity. In PASE, relative humidity dropped from 68% to 39% between 1,400 and 1,600 m. However, in both PEM-Tropics A and B, there is no measurable change between these two altitudes, as relative humidity remained in excess of 65%.

The model results for DMS and SO_2 shown in Fig. 1b correspond to the times and altitudes of the observational data. The “standard” REAM model was used here with BrO

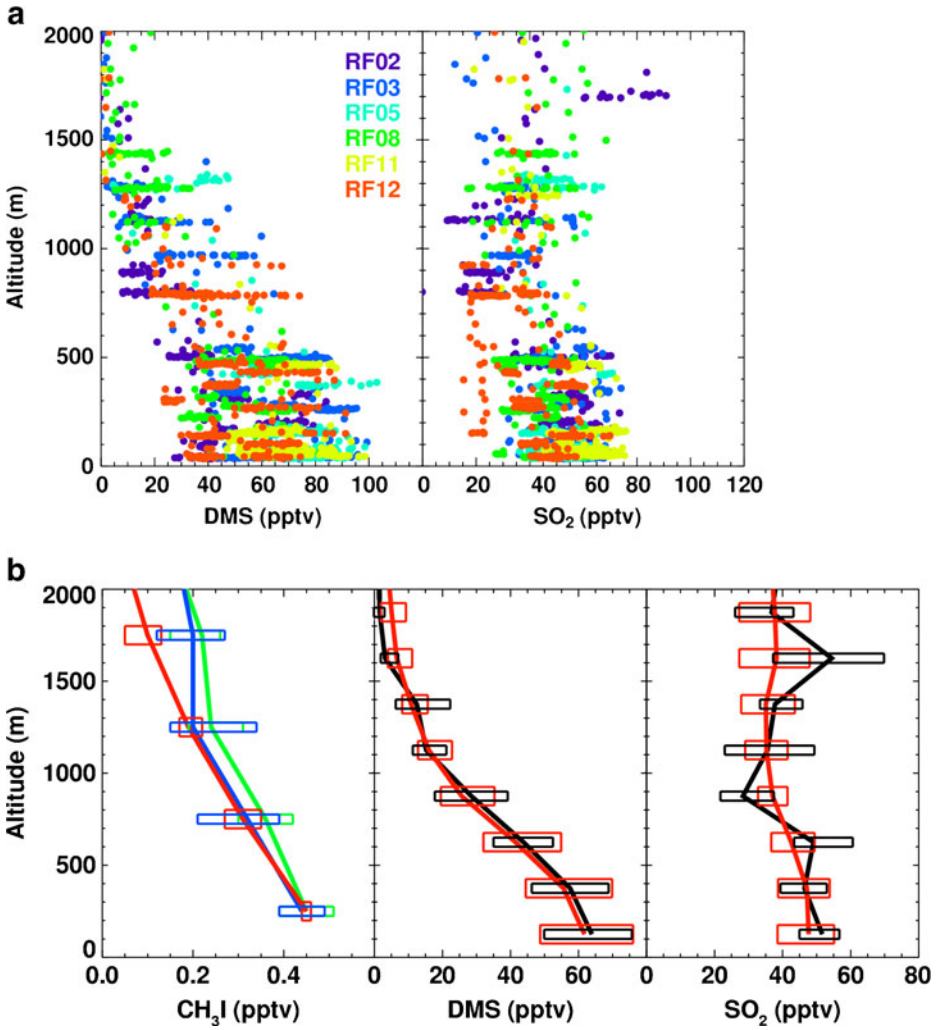

Fig. 1 **a**. DMS and SO_2 PASE observational raw data, with different colors reflecting different flights. b. Observed and simulated daytime median vertical profiles for CH_3I, DMS, and SO_2. The green, blue, and black lines are observation data for PEM-Tropics A, PEM-Tropics B, and PASE, respectively. The red lines are standard model data. Boxes indicate inner quartiles

levels set equal to zero. For DMS it is quite evident that the simulated median profile is in excellent agreement with those data generated during PASE over altitudes ranging from the ocean's surface up to the lower FT. This suggests that the BuL K_z value chosen (based on CH_3I profiles) was a reasonable approximation of the actual vertical mixing.

The model-estimated mean DMS flux was $2.0\pm0.4\times10^9$ molec $cm^{-2}s^{-1}$, which agrees quite well with the directly measured mean value of $1.9\pm0.4\times10^9$ molec $cm^{-2}s^{-1}$ reported by Conley et al. (2009). Although our results would seem to support Conley et al.'s assertion that no oxidants other than OH are required to explain the variability in DMS levels, as discussed later in the text, within the combined uncertainties of the measurements and model results, low levels of BrO cannot be ruled out.

The simulated SO_2 profile is also seen to be generally in good agreement with the observations, though the model does fail to reproduce the perturbations in SO_2 observed at mid-BuL altitudes and at 1,600 m. Whether these two departures are representative of the BuL environment depends a great deal on the robustness of the BuL and lower FT data sets. In this case, it is noteworthy that the PASE study was designed as a BL experiment; thus, the data reported here for altitudes corresponding to the BuL and FT are quite limited and therefore not necessarily representative of average conditions for these two altitude regimes.

As revealed in other earlier tropical sulfur studies (Bandy et al. 1996; Davis et al. 1999; and Nowak et al. 2001), DMS and SO_2 profiles typically exhibit a strong anticorrelation in their respective diurnal trends. From Fig. 2, this is again seen to be the case for the PASE study. Quite significant here is the fact that the model-predicted trends for these two species are in good agreement with the BL observations. The standard model does seem to slightly overestimate SO_2 losses; but the predicted profile is well within one quartile of the observational median. By comparison, at BuL altitudes the agreement is much worse (see Fig. 3). As mentioned previously, the BuL data set was quite limited in scope, and when combined with the natural variability expected in BuL conditions, these results are not that unexpected. For instance, the variability in relative humidity within the BuL was up to three times greater than in the BL during PASE. This has implications for the strength of convection within the BuL, as well as cloud coverage over this region, thereby impacting both DMS and SO_2 concentration levels. In spite of these difficulties, the DMS BuL profile clearly shows a negative trend from mid morning to late afternoon. For SO_2, the model-predicted profile again shows a slightly upward trend during the course of the day, though it is weaker than its counterpart, DMS.

4.2 BrO sensitivity tests

Previous field studies in which DMSO has been measured have led to speculation that BrO may be an important oxidant for DMS in the equatorial Pacific (Nowak et al. 2001). In addition, recent measurements in the equatorial Atlantic have shown that BrO in excess of 2 pptv (Read et al. 2008b) may be present in marine areas near upwelling regions. Unfortunately, no DMSO or BrO data were recorded during the PASE field study. In lieu of

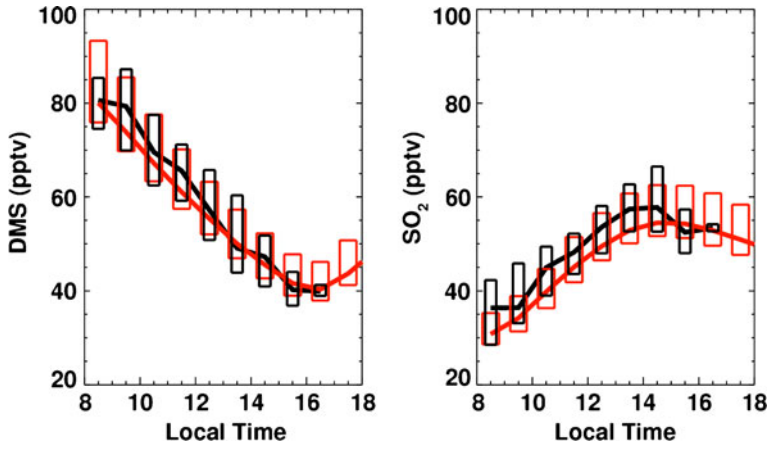

Fig. 2 Observed and simulated median hourly time series for DMS and SO_2 in the BL. Black lines are PASE observations, and the red lines are standard model data. Boxes indicate inner quartiles

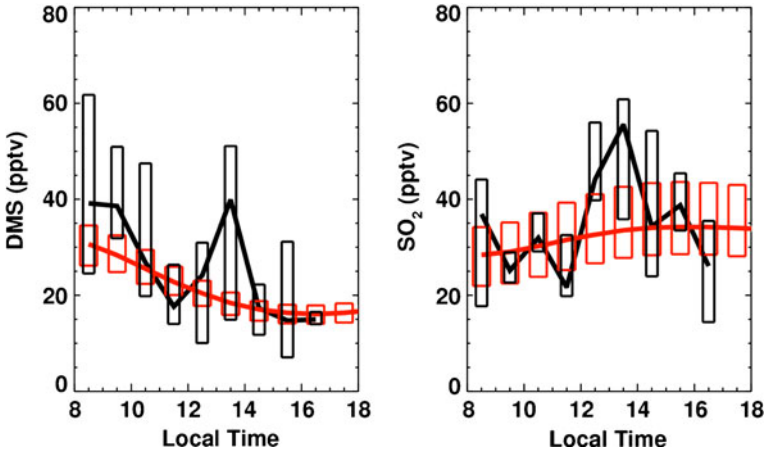

Fig. 3 Same as Fig. 2, but for the BuL

this, sensitivity calculations were carried out here in an effort to explore the possible impact of BrO on DMS chemistry. Earlier, the DMS flux was estimated based on only the oxidant OH, resulting in a value of $2.0\pm0.4\times10^9$ molec $cm^{-2}s^{-1}$. The DMS/OH conversion efficiency under these conditions has been estimated at ~73±3% (see further discussion in section 4.3).

In the current sensitivity test, a maximum value of 1 pptv of BrO was added to the modeled chemistry such that it defined the maximum high noon value for this diurnally varying species. The model results revealed that to maintain the same level of BL DMS, the flux for this species needed to be increased by ~14%, or to a new total of $2.3\pm0.4\times10^9$ molec $cm^{-2}s^{-1}$. This increase also leads to a somewhat lower total DMS-to-SO_2 conversion rate of 60±7% since the BrO reaction involves only the addition oxidation channel, thus leading to predominantly DMSO (Ingham et al. 1999). Furthermore, because the latter species results in virtually no generation of SO_2 under BL conditions (see detailed discussion in section 4.3), the calculated conversion efficiency must decrease. Even so, due to the fact that the DMS flux was increased, the addition of BrO at the 1 pptv level still has very little impact on the net production of SO_2. Although there remain significant uncertainties regarding several aspects of marine bromine chemistry, the current result suggests that, within the uncertainties of the PASE measurements and model results, some BrO oxidation of DMS cannot be ruled out.

4.3 SO_2 sensitivity to aerosol scavenging

Figure 4 shows the impact of sea-salt scavenging on the model-predicted altitude profile for SO_2. Quite noticeable here is the very modest difference between the profile generated from the standard model (red) and those runs having no sea-salt scavenging (green line). Interestingly, the observational data fall between these two lines. These results suggest that our standard model, using the Chameides and Stelson (1992) formulation for loss of SO_2 to sea salt, might slightly overestimate the role of sea-salt scavenging for SO_2. However, given the uncertainties in the measurements as well as in the model calculations, the agreement shown can be viewed as quite good. Overall, we estimate that 19% of the BL SO_2 is lost to sea-salt scavenging (Table 2).

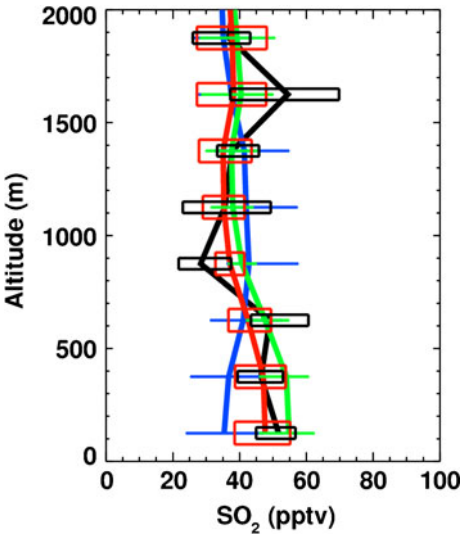

Fig. 4 Same as Fig. 1b for SO_2, with the addition of the median model profiles of enhanced sea-salt scavenging using the sea-salt flux by Clarke et al. (2006) (in blue) and no sea-salt scavenging (in green). Horizontal lines and boxes indicate inner quartiles

What is clearly outside any range of reasonable agreement is the profile shown when using the aerosol flux estimated by Clarke et al. (2006). This flux was based on a 10 m level wind speed of 8 m/s. The average wind speed observed during PASE was also 8 m/s. But in this case, even with BuL cloud scavenging turned off, BL SO_2 is underestimated by 30%. This suggests that if Clarke et al.'s aerosol flux is considered to be the most applicable to the PASE study, some other adjustment is needed in the model to bring SO_2 back in line. One possibility might involve lowering the aerosol alkalinity.

Also quite significant with regard to aerosol scavenging is the comparison between our PASE results and those reported by Faloona et al. (2010). The results from this study are

Table 2 Average SO_2 BL loss and formation rates and DMS fluxes from different studies

Study Location	Bandy et al. 1996	Yvon et al. 1996	Davis et al. 1999	Davis[a]	This Study 2010	Faloona et al. 2010
	Xmas Is.	12°S, 135°W	Xmas Is.	13°S, 142°W	PASE	PASE
Surface Dep.		58%	39%		48%	27%
Aerosol Scav.		37%	46%		19%	56%
OH oxidation		5%	15%		14%	10%
Transport to BuL		0	0		19%	7%
Total		100%	100%		100%	100%
SO_2 Formation						
Conv DMS $\rightarrow SO_2$	(62%[c] 65%[d])	40%[e]	72%[e]	(40–55%)	73%	near unity[f]
DMS Flux Est. (molec $cm^{-2}s^{-1}$)	3×10^9	11×10^9	2.3×10^9		2.0×10^9	1.9×10^9[g]

[a] Unpublished results, PEM-Tropics B, flight 16.

[b] Dry 28%, wet 9%.

[c] Range 43–85%, non-photochemical model assessment.

[d] Photochemical model derived conversion rate (Chen et al., 2000) based on Bandy et al. (1996) data.

[e] Average value (range 27–54%).

[f] Cited Range 90–129%.

[g] Direct measurements.

substantially lower than those reported by the above authors (e.g., 57%). Noteworthy here, however, is the fact that in the latter study, the authors have justified the "reasonableness" of a very large SO_2 aerosol sink by also estimating a very large conversion efficiency for DMS to SO_2, e.g., approaching unity. (For a comparison of conversion efficiencies and sea-salt scavenging values reported in other tropical sulfur studies, see Table 2.) Though interesting, this conclusion would seem to run contrary to all recently reported kinetic data, as well as contrary to the most recent results from other tropical field studies. For example, under tropical conditions, even one having no BrO, the OH oxidation of DMS proceeds by two channels, where ~75% occurs by abstraction and ~25% by addition (Sander et al. 2006). For the addition channel, only if the intermediate product DMSO is consumed by reaction with OH is there any possibility of generating SO_2. Even then, only if the resulting product from the DMSO/OH reaction, MSIA, is itself consumed by reaction with OH is there any possibility of forming an SO_2 product (Sander et al. 2006; Kukui et al. 2003). Although this sequence of reactions can be quite important under free tropospheric conditions (e.g., see DMS oxidation results reported by Arsene et al. 1999 involving an aerosol-free chamber), within the BL the competing reaction involving aerosol scavenging dominates (e.g., Henry's constant 1.0×10^7 $Matm^{-1}$, Campolongo et al. 1999). Furthermore, as demonstrated in recent field studies (Davis et al. 1998; Jefferson et al. 1998; Davis et al. 1999), the measured levels of MS in marine aerosols are inexplicably high when considering only the available gas-phase levels of MSA. In each of the above cases, only when DMSO was assumed to be rapidly scavenged by aerosols (with subsequent conversion to MS) were the observed elevated levels of MS understood. Confirming these field observations, laboratory studies have now shown that DMSO in the liquid phase is converted to MS (Zhu et al. 2006; Sehested and Holcman 1996; Scaduto 1995). In fact, in the most recent study by Zhu et al., the authors conclude that >97% of all MS found in the aerosol phase is formed in the liquid phase from organo-sulfur compounds. The above set of conclusions are also quite consistent with the still more recent sulfur field studies reported by Legrand et al. (2001) and Sciare et al. (2000), as discussed below in section 4.5.

Given the above setting, it is quite unlikely that DMSO formed in a tropical BL environment would yield significant SO_2. This leaves only the 75% abstraction channel as the single source of SO_2. However, even for this reaction channel, serious questions can be raised as to the efficiency with which the initially formed radical species (i.e., CH_3SCH_2) forms SO_2. Though the reaction kinetics for this species have not yet been fully documented, by analogy with OH-hydrocarbon reactions, this radical species is expected to react with O_2, producing the new radical CH_3SCH_2OO. Again, by analogy with alkyl peroxide reactions, under the low NO_x conditions of the tropics, this new radical species' tendency would be to react with the most abundant daytime HO_x radical available, HO_2. If so, the new species formed would be CH_3SCH_2OOH, a species that one might expect to have reasonable chemical stability. And even though this species has yet to be identified either in the field or laboratory, its physical characteristics would clearly include some degree of solubility in water. If so, this would again lead to yet another opportunity for a DMS oxidation product to be scavenged by marine aerosols. To the extent that this happens, the DMS-to-SO_2 conversion efficiency would be reduced still further. In this context, from an examination of the DMS-to-SO_2 conversion efficiencies reported in other tropical sulfur studies (Table 2), only Faloona et al.'s results suggest a different kind of chemistry may be happening. Approximately half report conversion values significantly below one of the most optimistic scenarios; namely, that all abstraction channel products convert to SO_2. Thus, at this time questions still remain regarding aspects of the conversion process. For example, speculation here is that future campaigns are likely to reveal that the

conversion rate itself may be found to be a function of several other atmospheric variables beyond just BrO. The list could include: NO_x, H_2O_2, and O_3 levels, as well as HO_x radical and aerosol loadings.

We note that the uncertainty cited here of ±3% for the conversion efficiency was that estimated by varying one of the most sensitive parameters in the model that impacts the conversion rate, i.e., aerosol surface area. In this case, model runs were made with the total aerosol surface area first increased by a factor of 2 and then decreased by a factor of 2. But even when making far more extreme chemical variations, it is quite difficult to increase the conversion efficiency to a level approaching 90%. As but one example: 1) reduce the aerosol surface area by a factor of 2; 2) then assume a 100% yield of SO_2 from the DMS-OH abstraction reaction; 3) also assume that the addition channel product DMSO, when it reacts with OH, forms MSIA with a 100% yield; and finally 4) also assume that when MSIA reacts with OH, it forms SO_2 with a 100% yield. The resulting DMS-to-SO_2 conversion efficiency from this analysis is still only 84%. As noted above, a critical element here is the strong tendency for DMSO and MSIA to be scavenged by marine aerosols, rather than to react with OH.

4.4 SO_2 sensitivity to other marine sulfur sources

Although the conversion rate of DMS to SO_2 appears to be bracketed within the range of 40 to 80% by observational field data, laboratory kinetic studies, and modeling assessments, these results do not preclude the possibility that observed SO_2 levels are influenced by still other primary marine sulfur sources. If this were the case, any estimate of the conversion rate based on observations of DMS and SO_2 alone could lead to the conclusion that the conversion rate was actually much higher than that cited above. In fact, they could reach levels of near 100%, or even higher, as recently suggested by Faloona et al. (2010). Earlier, Davis et al. (1999) and Nowak et al. (2001) independently raised this question as a result of what appeared then to be some atypical sulfur field observations. These two studies in the tropical Pacific were part of a larger field study sponsored by the NASA GTE program (e.g., PEM-Tropics A, 1996 and PEM-Tropics B, 1999).

In the case of the Davis et al. study, the suggestion of an additional sulfur source was made due to the model profile for SO_2 seemingly having a better fit with a DMS conversion efficiency in excess of 90%. However, these authors also pointed out that the reported diurnal sulfur results could just as easily be rationalized by assigning a more realistic uncertainty to the SO_2 data itself. They argued that a large uncertainty assignment could be justified due to the fact that atmospheric conditions, previous to the airborne data collection flight, had been greatly destabilized by convective activity in the sampling region. By contrast, in the study reported by Nowak et al., there were real-time data reported not only for DMS, SO_2, and OH, but for DMSO as well. It was the DMSO observations, in fact, that ultimately led to the hypothesis that an alternate (unknown) source of sulfur was a likely explanation for the atypical sulfur data reported in the PEM-Tropics B study. The specifics leading up to this conclusion involved the recording of a significant portion of a full diurnal BL profile during PEM-Tropics B flight 16. Thus, for all of the species listed above, significant portions of a diurnal profile were available for analysis. Interestingly, the geographical area sampled during flight 16 was again the tropical Pacific; however, in this case the location was downwind of the Marquesas Islands (9ºS). This area was quite near to where Yvon et al. (1996) had previously reported a shipboard marine sulfur study (see e.g., Table 2).

Quite surprising during flight 16 was the finding that daytime DMSO observations were ~5 times higher than predicted from a DMS oxidation box model (e.g., a chemical model similar to REAM, but without vertical transport). Even more surprising were the data collected under early-morning-dark conditions. These revealed DMSO values that were nearly two times higher than the daytime observations. By contrast, the modeled concentration level was estimated at near zero. All efforts to rectify this large disagreement using multiple versions of a conventional sulfur chemistry model, or by invoking other DMSO sources (i.e., BrO/DMS reactions producing DMSO directly), were unsuccessful. However, adding to this mystery were the still older Christmas Island DMSO data first reported by Bandy et al. (1996). In the latter case, DMSO levels were observed that exceeded model predictions by factors of 20 or more (Chen et al. 2000). And, once again, large values of DMSO were reported under nighttime conditions.

In sharp contrast to the anomalous DMSO PEM-Tropics B flight 16 results, a model assessment of the SO_2 and DMS data from this flight (D. Davis, unpublished results) were found to be generally inline with other tropical studies. For example, when the model was constrained by measured values of DMS and OH, the estimated DMS-to-SO_2 conversion efficiency ranged from 45–55% (see Table 2). Equally encouraging, the levels of MS observed were also inline with those predicted when assigning the OH/DMS addition channel to be 20% of the total oxidation, with its sequential products DMSO and MSIA being predominantly scavenged by aerosol and thus reacting heterogeneously (section 4.4).

The anomalously high PEM-Tropics B DMSO observations also turn out to be in conflict with two other independent studies by Legrand et al. (2001) in the Antarctic (85º S) and by Sciare et al. (2000) at Amsterdam Island (37º S). In both cases, DMS, DMSO, MSA, and MS were examined over a 1 month or longer time period. A critical finding in these studies was that the molar ratio of DMSO:DMS was typically in the range of 1 to 2.5%, as compared with the daytime results from PEM-Tropics B of ~5%, and those from the Christmas Island study (Bandy et al. 1996) of 19%. Equally significant, in the former two studies, DMSO levels at night were systematically lower than those observed during daylight hours, a result expected for a photochemically generated species.

The collective evidence, then, strongly suggests that a measurement problem(s), perhaps involving chemical interferants, may have given rise to the unusually high yields of DMSO in both the PEM-Tropics B flight 16 study and the Bandy et al. (1996) Christmas Island observations. However, until a systematic study of this species can be carried out in a tropical environment similar to that at Christmas Island, involving multiple DMSO measurement techniques, the possible role of non-DMS sulfur sources cannot be permanently tabled.

4.5 SO_2 sensitivity to dry deposition

Figure 5 illustrates the sensitivity of SO_2 levels to the value selected for dry deposition. In this simulation, we have carried out two types of runs; one using the dry deposition velocity estimated via the REAM model, and the other using an assumed value of zero, i.e., no SO_2 deposition. In general, the treatment of SO_2 as related to its loss to a water surface (effective Henry's constant is 4.5×10^7 $M atm^{-1}$) has been to view it as a water-soluble species having a deposition velocity similar to H_2SO_4. Here we have estimated this value at 0.71 $cm sec^{-1}$ based on an assumed ocean pH of 8.3. This REAM-calculated value is double the 0.36 cm sec^{-1} reported by Faloona et al., which involved a direct measurement. The results from the current study show that with a dry deposition value set equal to zero (green line), BL SO_2 increases by nearly 50%. This strongly suggests, then, that loss of SO_2 by dry deposition is a major BL sink for this species. Table 2, however, shows that different tropical studies

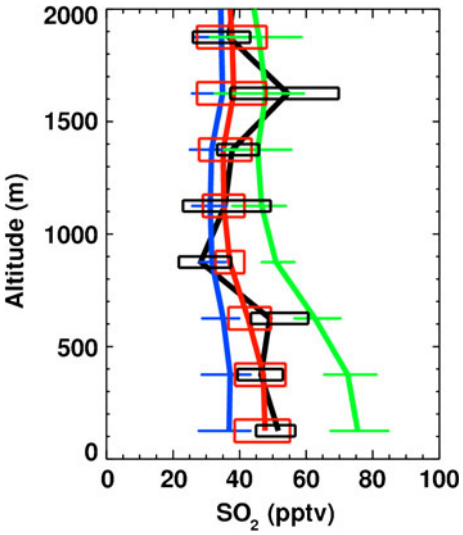

Fig. 5 Same as Fig. 4, except that the blue line is with modeled-derived SO_2 deposition velocity, and the green line is with no SO_2 dry deposition. In the standard model (red line), deposition velocity is a constant 0.36 cm/s. Horizontal lines and boxes indicate inner quartiles

have resulted in a rather wide range of estimated values for this loss pathway, e.g., a high of 58% to a low of 27%.

As shown in Table 5, yet another interesting comparison involving the deposition velocity of SO_2 is that of our REAM-estimated value versus that generated from the GEOS-Chem model. Recall, in the REAM "standard" model the dry deposition velocity is set by the PASE measurement because the resistance-in-series calculations yield values double that reported by Faloona et al. Here one can see that the GEOS-Chem model also predicts that SO_2 deposition is twice as fast as that derived from direct measurements recorded during PASE. Most global models like GEOS-Chem calculate the uptake of a soluble species by the ocean's surface based on the compound's effective Henry's law constant. These new deposition results suggest that, when addressing tropical BL conditions, global chemical models may need to reassess their formulations for calculating losses of soluble species to the ocean.

Tables 3 and 4 show the difference we now estimate in the respective budgets for sulfur in the BL and BuL. For example, in the BL, ~52% of the DMS is lost to oxidation by OH, with the remaining 48% being entrained into the BuL. Also, approximately half of the SO_2 in the BL is lost to dry deposition, while the remaining 52% is nearly evenly divided into entrainment to the BuL, oxidation by OH, and scavenging by sea-salt aerosol. In the BuL, 56% of the DMS is estimated as lost to reaction with OH, while the remaining 44% is transported to the lower FT. In the case of SO_2, cloud scavenging dominates as a sink, with 85% assigned to

Table 3 24-hour boundary layer budgets[a,b]

	Mean	Surf Flux[c]	BuL Flux	Chem Prod	Chem Loss	SS Scav
DMS	73(11)	5.6(1.0)	−2.7(0.7)	0	−2.9(0.4)	0
SO_2	43(6)	−1.0(0.2)	−0.4(0.2)	2.1(0.2)	−0.3(0.1)	−0.4(0.1)

[a] Mean mixing ratio in pptv. Flux, chemical production, loss, and sea-salt (SS) scavenging rates in pptv/hr. Negative values indicate sinks.

[b] Values in parentheses are one standard deviation.

[c] Positive surface flux indicates emission; negative surface flux indicates dry deposition.

Table 4 24-hour buffer layer budgets[a]

	Mean	BL Flux	FT Flux	Chem Prod	Chem Loss	Cloud Scav
DMS	32(12)	1.8(1.0)	−0.8(0.7)	0	−1.0(0.3)	0
SO_2	42(9)	0.4(0.3)	0.2(0.4)	0.7(0.2)	−0.2(0.0)	−1.1(0.8)

[a] The budget terms are defined as Table 1.

this process and only 15% being removed by OH oxidation. If we examine the combined BL/BuL, ~90% of the SO_2 source is from in-situ chemistry (DMS oxidation), with about ~10% coming from FT entrainment of SO_2. We have not quantified the potential impact of lateral advection on BL/BuL SO_2 as it is difficult to constrain 3-D model simulations using aircraft observations. However, Faloona et al. estimate that advection, on average, has no net impact on BL SO_2. The impact of advection on FT SO_2 is addressed in section 4.7.

A final comparison of our DMS and SO_2 results is that shown in Table 5. Here, the 1-D standard REAM model results are compared with those from the 3-D global GEOS-Chem model. In this case, it is quite evident that GEOS-Chem predicts a much shorter lifetime for SO_2 based on dry deposition. However, GEOS-Chem and REAM agree very well for SO_2 loss on sea-salt aerosols. Both models predict SO_2 oxidation by OH to be one of the smallest BL and BuL loss processes. Both also give nearly the same weight to the importance of cloud scavenging of SO_2 in the BuL.

Regarding the earlier discussion on the disparity between the directly measured dry deposition velocity of SO_2 versus that estimated from our model's use of resistance-in-series calculations, we do not have the necessary measurements from the PASE experiment to investigate at an appropriately detailed level the chemical/physical processes of SO_2 dry deposition. We speculate here on one factor that may be involved. That factor could involve shifts in the pH of ocean surface water, e.g., the ocean's surface microfilm. Given an average ocean pH of 8.3, the effective Henry's constant is 4.5×10^7 $M atm^{-1}$, and all ocean-surface resistance to SO_2 uptake effectively disappears. Thus, under these conditions, the SO_2 deposition velocity is very similar to most other highly soluble species (e.g., HNO_3, H_2SO_4). Thus, for the equatorial Pacific, the question that needs to be addressed is: What happens to the pH of the surface microfilm with continued long term exposure to acidic species? This could happen if the flux of DMS into the atmosphere were both steady and quite high in value, leading to a high, steady deposition of H_2SO_4 to the surface. If so, one interpretation of the measured deposition velocity of 0.36 $cm sec^{-1}$ is that this is a value that reflects an ocean surface pH that is closer to 5.0. Though, at first glance, such a large drop seems quite unlikely, this possibility needs further exploration before being completely dismissed.

Faloona et al. (2010) also considered the possibility of S(IV) saturation at the ocean surface being a means to explain the somewhat lower observed SO_2 dry deposition velocity. They found only one study that measured the sulfite concentration at the ocean surface (Campanella et al. 1995), and these results suggested sulfite levels that would be much lower than required for saturation. However, details regarding this study are lacking and again further study is needed.

4.6 SO_2 sensitivity to cloud scavenging

In the cloud sensitivity simulations (see Fig. 6), we contrast the level of SO_2 predicted in the BuL for the case where SO_2 cloud scavenging is removed with that given by our standard model. As seen in the figure, in the absence of cloud scavenging, the SO_2 vertical

Table 5 SO_2 lifetimes (hours) to chemical and physical sinks[a]

	REAM	GEOS-Chem
Boundary Layer SO_2 Sinks		
Deposition	42(6)	17
OH Oxidation	165(40)	150
SS Scav	118(26)	160
Buffer Layer SO_2 Sinks		
Cloud Scav	47(20)	46
OH Oxidation	237(58)	141

[a] Mean values with one standard deviation values in parentheses.

gradient within the BL becomes virtually flat. This can be contrasted to the results from the standard model (with scavenging) which shows a definite negative gradient. The latter behavior is generally in agreement with actual observational data, and suggests the existence of a strong BuL sink for SO_2. Interestingly, in the absence of cloud scavenging, there is also a 40–50% increase in the absolute level of BL SO_2. Indications are, then, that low-altitude clouds in the BuL can serve as a highly effective sink for BL-generated SO_2.

4.7 SO_2 in the lower free troposphere: local convection versus long-range transport

As mentioned earlier, SO_2, as treated in the standard REAM model, is fixed to the observed PASE value at 2 km. Without this fix value, the model underestimates observed SO_2 at that altitude by about 50% (Fig. 7). However, this raises the question of whether the REAM model is underestimating the impact of local convection, or if this additional SO_2 is being transported to the PASE sampling region from afar.

To address this issue, we initially increased the WRF-derived shallow convection by approximately a factor of 5. The results showed that, indeed, this enhancement improved the REAM prediction at 2 km (Fig. 7). However, there are at least two reasons for believing that this approach is not representative of actual conditions. First, by increasing local shallow convection, DMS also increases in the lower FT. In this case, the model run

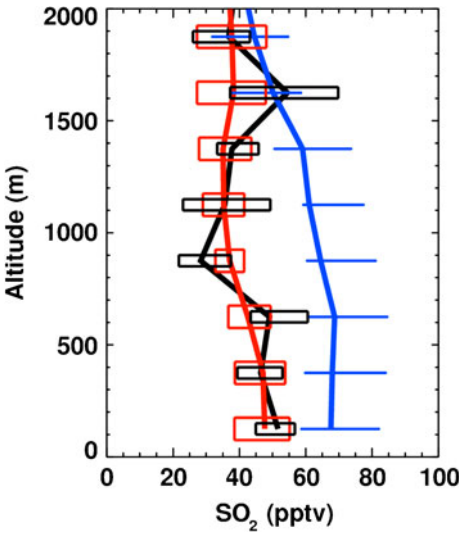

Fig. 6 Same as Fig. 1b for SO_2, with the addition of the median model profile without BuL cloud scavenging (in blue). Horizontal lines and boxes indicate inner quartiles

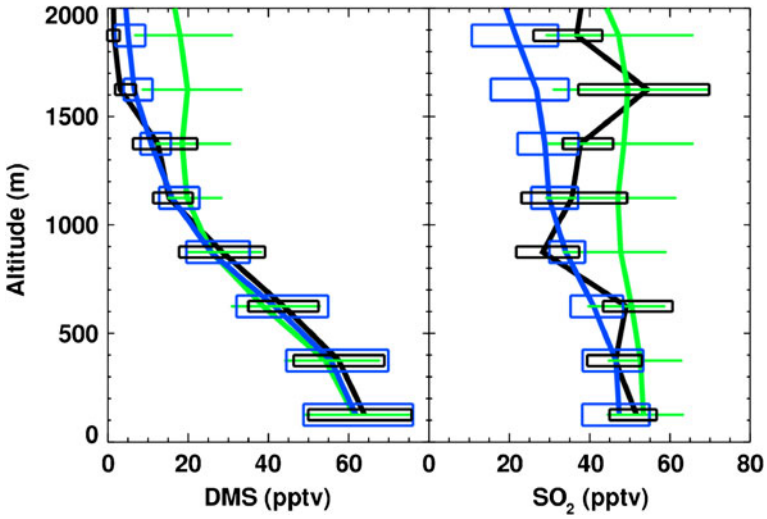

Fig. 7 Observed and simulated daytime median vertical profiles for DMS and SO_2. The black lines are PASE observation data. The blue lines are standard model data, but without the FT SO_2 source. The green lines are the same as the blue, but with WRF convection enhanced by a factor of 5. Horizontal lines and boxes indicate inner quartiles

predicts levels of 17 pptv, as compared to the observed value of ~5 pptv. Second, increasing local convection removes virtually all of the gradient in the vertical profile for SO_2. In the standard model (Fig. 1b), SO_2 shows a decrease from the BL to the BuL, before increasing slightly in the lower FT. These trends are generally consistent with PASE observations. With enhanced local convection, no gradient is evident as a function of altitude.

Given the above result, our effort was directed towards exploring the possibility that the elevated SO_2 in the lower FT was the byproduct of long-range transport. This long-range transport could be associated with DMS sources further to the east of the PASE sampling region, but still well within the equatorial upwelling region; or it could involve sources still further to the east, and thus reflect South American pollution. In the text that follows, we first examine what we believe to be the higher probability source, that involving DMS emissions to the east. In this scenario, the region from which the airmass advected would need to have much higher levels of SO_2 than typically observed during PASE. Thus, to examine this possibility, monthly-averaged fields for the month of August 2007 were acquired for three critical parameters: sea-surface temperature (SST), ocean-surface chlorophyll levels, and cloud-top temperatures. As shown in Fig. 8, superimposed on these fields is a red box denoting the PASE sampling region, along with three seven-day air back-trajectories, each having a starting altitude of 1,600 m, but with several different starting latitudes. These back-trajectories are the average of 31 seven-day runs, one set for each day of the month.

From the SST plot, a clear "tongue" of upwelling water can be seen around the equator, with the coolest waters being to the east of the PASE region. This potentially defines, then, a region that could have enhanced DMS emissions. The air back-trajectories also suggest that air parcels from this region were advected to the PASE region over a time period of approximately one week. The corresponding transit time was approximately equal to one lifetime for SO_2 if the oxidation by OH occurred under FT conditions.

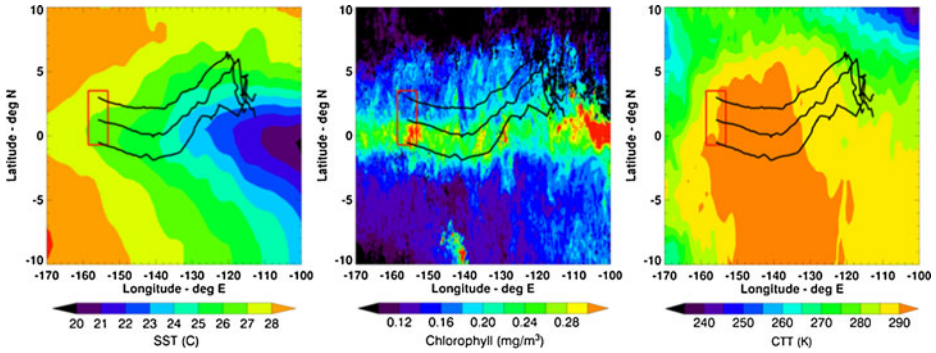

Fig. 8 **a** Monthly-mean sea-surface temperature (SST), **b** chlorophyll concentration, and c) cloud-top temperature (CTT) for August 2007. Data sources are described in section 2.3. Seven-day HYSPLIT median back-trajectories for the month of August are overlaid (the starting altitude for back-trajectories is 1,600 m). The red box indicates the PASE measurement region

Inspection of the chlorophyll map discloses that, at that time, there was clearly a region with elevated biogenic activity centered near the equator. Although not proof of higher emission rates of DMS (see Observations section 2.3), it is encouraging that a region can be identified having high potential for enhanced DMS emissions. In conjunction with the air back-trajectories, which suggest that air from this area reached the PASE sampling region in less than one week, the only remaining requirement is that of having a mechanism for moving DMS emissions from the BL to the FT. In this case, the cloud-top temperature distribution for the region has proven helpful. From Fig. 8, it can be seen that cloud-top temperatures in the area of high upwelling/biological activity are 5–15° cooler than in the PASE region. This suggests that the region to the east was substantially more active in terms of convection than was the PASE sampling area. Thus, based on all available input, it appears likely that long-range transport of SO_2 into the PASE sampling area occurred from a region ~4,200 km to the east.

The possibility that the transport of sulfur may have come from an even greater distance (e.g., the coast of South America), as suggested by Faloona et al., cannot be ruled out. However, it is noteworthy that during the PEM-Tropics A and B programs, which sampled along the west coast of South America, as well as in the equatorial Pacific region, little evidence of a major sulfur source from South America was evident over a two to three week time period.

5 Conclusions

Field measurements from the 2007 PASE study, which focused on DMS emission fluxes and SO_2 formation and losses, have provided important new observational constraints on marine sulfur chemistry over equatorial regions. PASE is the first field experiment in which simultaneous measurements were made of the DMS emission flux from and SO_2 deposition flux to the ocean's surface. These observations, together with in-situ measurements of DMS, SO_2, and OH in the BL, BuL, and lower FT, have greatly facilitated the refinement of current photochemical models designed to address the role of DMS in controlling atmospheric sulfur levels under tropical conditions. In particular, they have clearly identified the importance of vertical transport in linking the chemical and physical processes in the BL, BuL, and lower FT. Consequently, we have applied a state-of-the-

science 1-D chemical transport model (REAM) to address major issues related to the marine sulfur budget.

Specific findings included: 1) In the absence of any oxidant other than OH, the DMS-to-SO_2 conversion efficiency was evaluated at ~73%; 2) the addition of BrO at levels of 1 pptv resulted in an estimated increase in the marine flux of DMS by ~14% and decreased the overall DMS-to-SO_2 conversion efficiency to 60%; 3) BL SO_2 losses consisted of 48% dry deposition, 19% aerosol scavenging, 19% transport to the BuL, and 14% OH oxidation. In sharp contrast, BuL SO_2 losses consisted of 85% cloud scavenging and 15% OH oxidation.

PASE measurements of the dry deposition velocity for SO_2 were approximately one-half that predicted by the resistance-in-series scheme used in the REAM and GEOS-Chem models. The specific process or processes responsible for this difference have not been identified from the PASE data. Speculation here is that it may involve the presence of a steady source of DMS oxidation products to the ocean's surface microfilm layer. The argument would be that this steady influx of acidic species might shift the pH of this layer, thereby changing the actual deposition flux.

Finally, as related to observations showing elevated FT levels of SO_2 in the PASE sampling area, it appears likely that long-range transport was a major factor. This conclusion was based on analysis of SST distributions, biogenic activity, and cloud top temperature data in conjunction with air back-trajectory projections. Thus, it now appears that an intense DMS source region ~4,200 km to the east of the PASE sampling area may have been responsible.

Acknowledgements This work was made possible by a grant from the atmospheric chemistry program of the National Science Foundation (grant #ATM-0627227) through a subcontract from Drexel University to the Georgia Institute of Technology. We thank Gao Chen for his help in developing aspects of the sulfur model. The authors gratefully acknowledge the NOAA Air Resources Laboratory (ARL) for the provision of the HYSPLIT transport and dispersion model and READY website (http://www.arl.noaa.gov/ready.php) used in this publication. Ozone data are from I.B. Pollack, T.L. Campos, and A.J. Weinheimer.

References

Alexander, B., Park, R.J., Jacob, D.J., Li, Q.B., Yantosca, R.M., Savarino, J., Lee, C.C.W., Thiemens, M.H.: Sulfate formation in sea-salt aerosols: Constraints from oxygen isotopes. J. Geophys. Res. Atmos. **110** (D10), D10307 (2005). doi:10.1029/2004JD005659

Andreae, M.O., Raemdonck, H.: Dimethyl sulfide in the surface ocean and the marine atmosphere: a global view. Science **221**, 744–747 (1983)

Andreae, M.O., Elbert, W., de Mora, S.J.: Biogenic sulfur emissions and aerosols over the tropical South Atlantic – 3. Atmospheric dimethylsulfide, aerosols, and cloud condensation nuclei. J. Geophys. Res. **100**(D6), 11335–11356 (1995)

Arsene, C., Barnes, I., Becker, K.H.: FT-IR product study of the photo-oxidation of dimethyl sulfide: temperature and O_2 partial pressure dependence. Phys. Chem. Chem. Phys. **1**, 5463–5470 (1999)

Arsene, C., Barnes, I., Becker, K.H., Schneider, W.F., Wallington, T.T., Mihalopoulos, N., Patroescu-Klotz, J. V.: Formation of methane sulfinic acid in the gas-phase OH-radical initiated oxidation of dimethyl sulfoxide. Environ. Sci. Technol. **36**, 5155–5163 (2002)

Bandy, A., Thornton, D.C., Blomquist, B.W., Chen, S., Wade, T.P., Ianni, J.C., Mitchell, G.M., Nadler, W.: Chemistry of dimethyl sulfide in the equatorial Pacific atmosphere. Geophys. Res. Lett. **23**(7), 741–744 (1996)

Bandy, A.R., Thornton, D.C., Tu, F.H., Blomquist, B.W., Nadler, W., Mitchell, G.M., Lenschow, D.H.: Determination of the vertical flux of dimethyl sulfide by eddy correlation and atmospheric pressure ionization mass spectrometry (APIMS). J. Geophys. Res. **107**(D24), 4743 (2002). doi:10.1029/2002JD002472

Barnes, I., Bastian, V., Becker, K., Overath, R.: Kinetic studies of the reactions of IO, BrO, and ClO with dimethylsulfide. Int. Jour. Chem. Kin. **23**, 579–591 (1991)

Barone, S.B., Turnipseed, A.A., Ravishankara, A.R.: Reaction of OH with dimethyl sulfide (DMS). 1. Equilibrium constant for OH + DMS reaction and the kinetics of the OH-DMS + O_2 reaction. J. Phys. Chem. **100**, 14694–14702 (1996)

Berglen, T.F., Berntsen, T.K., Isaksen, I.S.A., Sundet, J.K.: A global model of the coupled sulfur/oxidant chemistry in the troposphere: the sulfur cycle. J. Geophys. Res. Atmos. **109**(D19), D19310 (2004). doi:10.1029/2003JD003948

Blomquist, B.W., Fairall, C.W., Huebert, B.J., Kieber, D.J., Westby, G.R.: DMS sea-air transfer velocity: direct measurements by eddy covariance and parameterization based on the NOAA/COARE gas transfer model. Geophys. Res. Lett. **33**(7), L07601 (2006). doi:10.1029/2006GL025735

Campanella, L., Cipriani, P., Martini, T.M., Sammartino, M.P., Tomassetti, M.: New enzyme sensor for sulfite analysis in sea and river water samples. Anal. Chim. Acta **305**(1–3), 32–41 (1995)

Campolongo, F., Saltelli, A., Jensen, N.R., Wilson, J., Hjorth, J.: The role of multiphase chemistry in the oxidation of dimethylsulfide (DMS): a latitude dependent analysis. J. Atmos. Chem. **32**, 327–356 (1999)

Chameides, W.L., Stelson, A.W.: Aqueous-phase chemical processes in deliquescent sea-salt aerosols: a mechanism that couples the atmospheric cycles of S and sea salt. J. Geophys. Res. Atmos. **97**(D18), 20565–20580 (1992)

Charlson, R.J., Lovelock, J.E., Andreae, M.O., Warren, S.G.: Oceanic phytoplankton, atmospheric sulfur, cloud albedo and climate. Nature **326**, 655–661 (1987)

Chen, G., Davis, D.D., Kasibhatla, P., Bandy, A.R., Thornton, D.C., Huebert, B.J., Clarke, A.D., Blomquist, B.W.: A study of DMS oxidation in the tropics: comparison of christmas island field observations of DMS, SO_2, and DMSO with model simulations. J. Atmos. Chem. **37**(2), 137–160 (2000)

Choi, Y., Wang, Y., Zeng, T., Martin, R.V., Kurosu, T.P., Chance, K.: Evidence of lightning NO_x and convective transport of pollutants in satellite observations over North America. Geophys. Res. Lett. **32** (2), L02805 (2005). doi:10.1029/2004GL021436

Choi, Y., Wang, Y., Zeng, T., Cunnold, D., Yang, E., Martin, R., Chance, K., Thouret, V., Edgerton, E.: Springtime transitions of NO2, CO, and O3 over North America: model evaluation and analysis. J. Geophys. Res. **113**(D20), D20311 (2008a). doi:10.1029/2007JD009632

Choi, Y., Wang, Y., Yang, Q., Cunnold, D., Zeng, T., Shim, C., Luo, M., Eldering, A., Bucsela, E., Gleanson, J.: Spring to summer northward migration of high O3 over the western North Atlantic. Geophys. Res. Lett. **35**(4), L04818 (2008b). doi:10.1029/2007GL032276

Clarke, A.D., Davis, D., Kapustin, V.N., Eisele, F., Chen, G., Paluch, I., Lenschow, D., Bandy, A.R., Thornton, D., Moore, K., Mauldin, L., Tanner, D., Litchy, M., Carroll, M.A., Collins, J., Albercook, G.: Particle nucleation in the tropical boundary layer and its coupling to marine sulfur sources. Science **282**, 89–92 (1998)

Clarke, A.D., Shinozuka, Y., Kapustin, V.N., Howell, S., Huebert, B., Doherty, S., Anderson, T., et al.: Size distributions and mixtures of dust and black carbon aerosol in Asian outflow: physiochemistry and optical properties. J. Geophys. Res. **109**(D15), D15S09 (2004). doi:10.1029/2003JD004378

Clarke, A.D., Owens, S.R., Zhou, J.C.: An ultrafine sea-salt flux from breaking waves: implications for cloud condensation nuclei in the remote marine atmosphere. J. Geophys. Res. Atmos. **111**(D6), D06202 (2006). doi:10.1029/2005JD006565

Conley, S.A., Faloona, I., Miller, G.H., Lenschow, D.H., Blomquist, B., Bandy, A.: Closing the dimethyl sulfide budget in the tropical marine boundary layer during the pacific atmospheric sulfur experiment. Atmos. Chem. Phys. **9**, 8745–8756 (2009)

Corbett, J.J., Fischbeck, P.S., Pandis, S.N.: Global nitrogen and sulfur inventories for oceangoing ships. J. Geophys. Res. **104**(D3), 3457–3470 (1999)

Davis, D.D., Chen, G., Kasibhatla, P., Jefferson, A., Tanner, D., Eisele, F., Lenschow, D., Neff, W., Berresheim, H.: DMS oxidation in the Antarctic marine boundary layer: Comparison of model simulations and field observations of DMS, DMSO, $DMSO_2$, H_2SO_4 (g), MSA (g), and MSA (p). J. Geophys. Res. **103**(D1), 1657–1678 (1998)

Davis, D., Chen, G., Bandy, A., Thornton, D., Eisele, F., Mauldin, L., Tanner, D., Lenschow, D., Fuelberg, H., et al.: Dimethyl sulfide oxidation in the equatorial Pacific: comparison of model simulations with field observations for DMS, SO_2, H_2SO_4(g), MSA(g), MS, and NSS. J. Geophys. Res. Atmos. **104**(D5), 5765–5784 (1999)

Draxler, R.R., Rolph, G.D.: HYSPLIT (HYbrid Single-Particle Lagrangian Integrated Trajectory) Model access via NOAA ARL READY Website (http://ready.arl.noaa.gov/HYSPLIT.php). NOAA Air Resources Laboratory, Silver Spring, MD (2010)

Dyke, J., Ghosh, M., Goubet, M., Lee, E., Levita, G., Miqueu, K., Shallcross, D.: A study of the atmospherically relevant reaction between molecular chlorine and dimethylsulfide (DMS): establishing

the reaction intermediate and measurement of absolute photoionization cross-sections. Chem. Phys. **324**, 85–95 (2006)
Fairall, C.W., Hare, J.E., Edson, J.B., McGillis, W.: Parameterization and micrometeorological measurement of air-sea gas transfer. Bound. Layer Meteor. **96**, 63–105 (2000)
Faloona, I.: Sulfur processing in the marine atmospheric boundary layer: a review and critical assessment of modeling uncertainties. Atmos. Environ. **43**, 2841–2854 (2009)
Faloona, I., Conley, S.A., Blomquist, B., Clarke, A.D., Kapustin, V., Howell, S., Lenschow, D.H., Bandy, A. R.: Sulfur dioxide in the tropical marine boundary layer: dry deposition and heterogeneous oxidation observed during the Pacific Atmospheric Sulfur Experiment. J. Atmos. Chem. (2010). doi:10.1007/s10874-010-9155-0
Fountoukis, C., Nenes, A.: ISORROPIA II: A computationally efficient thermodynamic equilibrium model for K^+ -Ca^{2+} -Mg^{2+} -NH_4^+ -Na^+ -SO_4^{2-}-NO_3—Cl^--H2O aerosols. Atmos. Chem. Phys. **7**, 4639–4659 (2007)
Gershenzon, M., Davidovits, P., Jayne, J.T., Kolb, C.E., Worsnop, D.R.: Simultaneous uptake of DMS and ozone on water. J. Phys. Chem. A **105**, 7031–7036 (2001)
Ghan, S.J., Taylor, K.E., Penner, J.E.: Model test of CCN-cloud albedo climate forcing. Geophys. Res. Lett. **17**(5), 607–610 (1990)
Gurciullo, C., Lerner, B., Sievering, H., Pandis, S.N.: Heterogeneous sulfate production in the remote marine environment: Cloud processing and sea-salt particle contributions. J. Geophys. Res. Atmos. **104**(D17), 21719–21731 (1999)
Hegg, D.A., Radke, L.F., Hobbs, P.V.: Particle production associated with marine clouds. J. Geophys. Res. **95**(D9), 13917–13926 (1990)
Huebert, B.J., Howell, S., Laj, P., Johnson, J.E., Bates, T.S., Quinn, P.K., Yegorov, V., Clarke, A.D., Porter, J.N.: Observations of the atmospheric sulfur cycle on SAGA-3. J. Geophys. Res. **98**(D9), 16985–16996 (1993)
Huebert, B.J., Blomquist, B.W., Hare, J.E., Fairall, C.W., Johnson, J.E., Bates, T.S.: Measurement of the sea-air DMS flux and transfer velocity using eddy correlation. Geophys. Res. Lett. **31**(23), L23113 (2004). doi:10.1029/2004GL021567
Hynes, A., Wine, P., Semmes, D.: Kinetics and mechanisms of OH reactions with organic sulfides. J. Phys. Chem. **90**, 4148–4156 (1986)
Ingham, T., Bauer, D., Sander, R., Crutzen, P., Crowley, J.: Kinetics and products of the reactions of BrO + DMS and Br + DMS at 298 K. J. Phys. Chem. **103**, 7199–7209 (1999)
Jaeglé, L., et al.: Global sea salt emissions: New constraints from in situ, AERONET, and MODIS observations, in preparation for submission to Atmos. Chem. Phys. Discuss. (2010)
Jefferson, A., Tanner, D.J., Eisele, F.L., Huey, J.W., Davis, D.D., Chen, G., Torres, A., Berresheim, H.: OH oxidation chemistry and MSA formation in the coastal Antarctic boundary layer. J. Geophys. Res. **103** (D1), 1647–1656 (1998)
Kettle, A.J., Andreae, M.O., Amouroux, D., Andreae, T.W., Bates, T.S., Berresheim, H., Bingemer, H., Boniforti, R., et al.: A global database of sea surface dimethylsulfide (DMS) measurements and a procedure to predict sea surface DMS as a function of latitude, longitude, and month. Global Bio. Cycles **13**(2), 399–444 (1999)
Kloster, S., Feichter, J., Reimer, E.M., Six, K.D., Stier, P., Wetzel, P.: DMS cycle in the marine ocean-atmosphere system – a global model study. Biogeosciences **3**(1), 29–51 (2006)
Koch, D., Schmidt, G.A., Field, C.V.: Sulfur, sea salt, and radionuclide aerosols in GISS ModelE. J. Geophys. Res. Atmos. **111**(D6), D06206 (2006). doi:10.1029/2004JD005550
Kritz, M.A.: Exchange of sulfur between the free troposphere, marine boundary layer, and the sea surface. J. Geophys. Res. **87**(C11), 8795–8803 (1982)
Kukui, A., Borissenko, D., Laverdet, G., Le Bras, G.: Gas-phase reactions of OH radicals with dimethyl sulfoxide and methane sulfinic acid using turbulent flow reactor and chemical ionization mass spectrometry. J. Phys. Chem. A **107**, 5732–5742 (2003)
Lee, Y.N., Zhou, X.: Aqueous reaction kinetics of ozone and dimethylsulfide and its atmospheric importance. J. Geophys. Res. **99**(D2), 3597–3605 (1994)
Legrand, M., Sciare, J., Jourdain, B., Genthon, C.: Subdaily variations of atmospheric dimethylsulfide, dimethylsulfoxide, methanesulfonate, and non-seasalt sulfate aerosols in the atmospheric boundary layer at Dumont d'Urville (coastal Antarctica) during summer. J. Geophys. Res. Atmos. **106**(D13), 14409–14422 (2001)
Liu, X.H., Penner, J.E., Das, B.Y., Bergmann, D., Rodriguez, J.M., Strahan, S., Wang, M.H., Feng, Y.: Uncertainties in global aerosol simulations: Assessment using three meteorological data sets. J. Geophys. Res. Atmos. **112**(D11), D11212 (2007). doi:10.1029/2006JD008216
Lovelock, J.E., Maggs, R.J., Rasmussen, R.A.: Atmospheric dimethyl sulphide and the natural sulphur cycle. Nature **237**, 452–453 (1972)
Mauldin III, R.L., Frost, G.J., Chen, G., Tanner, D.J., Prevot, A.S.H., Davis, D.D., Eisele, F.L.: OH measurements during the first aerosol characterization experiment (ACE 1): observations and model comparisons. J. Geophys. Res. Atmos. **103**(D13), 16713–16729 (1998)

Mauldin III, R.L., Tanner, D.J., Heath, J.A., Huebert, B.J., Eisele, F.L.: Observations of H_2SO_4 and MSA during PEM-Tropics A. J. Geophys. Res. **104**(D5), 5801–5816 (1999)

Nowak, J.B., Davis, D.D., Chen, G., Eisele, F.L., Mauldin III, R.L., Tanner, D.J., Cantrell, C., Kosciuch, E., Bandy, A., Thornton, D., Clarke, A.: Airborne observations of DMSO, DMS, and OH at marine tropical latitudes. Geophys. Res. Lett. **28**(11), 2201–2204 (2001)

Park, R.J., Jacob, D.J., Field, B.D., Yantosca, R.M., Chin, M.: Natural and transboundary pollution influences on sulfate-nitrate-ammonium aerosols in the United States: implications for policy. J. Geophys. Res. **109**(D15), D15204 (2004). doi:10.1029/2003JD004473

Petelski, T.: Marine aerosol fluxes over open sea calculated from vertical concentration gradients. J. Aerosol Sci. **34**, 359–371 (2003)

Read, K.A., Lewis, A.C., Bauguitte, S., Rankin, A.M., Salmon, R.A., Wolff, E.W., Saiz-Lopez, A., Bloss, W. J., Heard, D.E., Lee, J.D., Plane, J.M.C.: DMS and MSA measurements in the Antarctic boundary layer: impact of BrO on MSA production. Atmos. Chem. Phys. **8**, 2985–2997 (2008a)

Read, K.A., Mahajan, A.S., Carpenter, L.J., Evans, M.J., Faria, B.V.E., Heard, D.E., Hopkins, J.R., Lee, J.D., et al.: Extensive halogen-mediated ozone destruction over the tropical Atlantic Ocean. Nature **453**(7199), 1232–1235 (2008b). doi:10.1038/nature07035

Ridley, B.A., Grahek, F.E., Walega, J.G.: A small, high-sensitivity, medium-response ozone detector for measurements from light aircraft. J. Atmos. Oceanic Tech. **9**, 142–148 (1992)

Rolph, G.D.: Real-time Environmental Applications and Display sYstem (READY) Website (http://ready.arl.noaa.gov). NOAA Air Resources Laboratory, Silver Spring, MD (2010)

Russell, L.M., Lenschow, D.H., Laursen, K.K., Krummel, P.B., Siems, S.T., Bandy, A.R., Thornton, D.C., Bates, T.S.: Bidirectional mixing in an ACE 1 marine boundary layer overlain by a second turbulent layer. J. Geophys. Res. Atmos. **103**(D13), 16411–16432 (1998)

Saiz-Lopez, A., Mahajan, A.S., Salmon, R.A., Bauguitte, S.J.B., Jones, A.E., Roscoe, H.K., Plane, J.M.C.: Boundary layer halogens in coastal Antarctica. Science **317**, 348–351 (2007)

Sander, S., Golden, D., Kurylo, M., Moortgat, G., Wine, P., Ravishankara, A., Kolb, C., Molina, M., Finlayson-Pitts, B., Huie, R.: Chemical kinetics and photochemical data for use in atmospheric studies, evaluation number 15. JPL Publication 06-2 (2006)

Scaduto, R.C.: Oxidation of DMSO and methanesulfinic acid by the hydroxyl radical. Free Radical Biol. Med. **18**, 271–277 (1995)

Sciare, J., Kanakidou, M., Mihalopoulos, N.: Diurnal and seasonal variations of atmospheric dimethylsuloxide at Amsterdam Island in the southern Indian Ocean. J. Geophys. Res. Atmos. **105**(D13), 17257–17265 (2000)

Sehested, K., Holcman, J.: A pulse radiolysis study of the OH radical induced autoxidation of methanesulfinic acid. Radiat. Phys. Chem. **47**, 357–360 (1996)

Seinfeld, J., Pandis, S.: Atmospheric chemistry and physics: From air pollution to climate change. Wiley, New York (1998)

Skamarock, W.C., Klemp, J.B., Dudhia, J., Gill, D.O., Barker, D.M., Wang, W., Powers, J.G.: A description of the advanced research WRF version 2. NCAR Tech. Note (2005)

Slinn, S.A., Slinn, W.G.N.: Modeling of atmospheric particulate deposition to natural waters. Atmospheric Pollutants in Natural Waters, 23-53, Ed. S. J. Eisenreich. Ann Arbor. Sci., Michigan (1981)

Smith, M.H., Park, P.M., Consterdine, I.E.: Marine aerosol concentrations and estimated fluxes over the sea. Q. J. R. Meteorol. Soc. **119**, 809–824 (1993)

Thomas, M.A., Suntharalingam, P., Pozzoli, L., Rast, S., Devasthale, A., Kloster, S., Feichter, J., Lenton, T. M.: Quantification of DMS aerosol-cloud-climate interactions using the ECHAM5-HAMMOZ model in a current climate scenario. Atmos. Chem. Phys. **10**, 7425–7438 (2010)

Thornton, D.C., Bandy, A.R., Tu, F.H., Blomquist, B.W., Mitchell, G.M., Nadler, W., Lenschow, D.H.: Fast airborne sulfur dioxide measurements by Atmospheric Pressure Ionization Mass Spectrometry (APIMS). J. Geophys. Res. Atmos. **107**(D22), 4632 (2002). doi:10.1029/2002JD002289

Urbanski, S.P., Stickel, R.E., Wine, P.H.: Mechanistic and kinetic study of the gas-phase reaction of hydroxyl radical with dimethyl sulfoxide. J. Phys. Chem. A **102**, 10522–10529 (1998)

Verma, S., Boucher, O., Reddy, M.S., Upadhyaya, H.C., Le Van, P., Binkowski, F.S., Sharma, O.P.: Modeling and analysis of aerosol processes in an interactive chemistry general circulation model. J. Geophys. Res. Atmos. **112**(D3), D03207 (2007). doi:10.1029/2005JD006077

Wang, Y., Jacob, D.J., Logan, J.A.: Global simulation of tropospheric O_3-NO_x-hydrocarbon chemistry. 1. Model formulation. J. Geophys. Res. **103**(D9), 10713–10725 (1998)

Wang, Y., Liu, S.C., Hongbin, Y., Sandholm, S.T., Chen, T., Blake, D.R.: Influence of convection and biomass burning outflow on tropospheric chemistry over the tropical Pacific. J. Geophys. Res. **105**(D7), 9321–9333 (2000)

Wang, Y., Liu, S.C., Wine, P.H., Davis, D.D., Sandholm, S.T., Atlas, E.L., Avery, M.A., Blake, D.R., Blake, N.J., Brune, W.H., et al.: Factors controlling tropospheric O_3, OH, NO_x, and SO_2 over the tropical Pacific during PEM-Tropics B. J. Geophys. Res. Atmos. **106**(D23), 32733–32747 (2001)

Wang, Y., Choi, Y., Zeng, T., Ridley, B., Blake, N., Blake, D., Flocke, F.: Late-spring increase of trans-Pacific pollution transport in the upper troposphere. Geophys. Res. Lett. **33**(1), L01811 (2006). doi:10.1029/2005GL024975

Wang, Y., Choi, Y., Zeng, T., Davis, D., Buhr, M., Huey, L.G., Neff, W.: Assessing the photochemical impact of snow NO_x emissions over Antarctica during ANTCI 2003. Atmos. Environ. **42**, 2849–2863 (2008)

Weber, R.J., Moore, K., Kapustin, V., Clarke, A., Mauldin, R.L., Kosciuch, E., Cantrell, C., Eisele, F., Anderson, B., Thornhill, L.: Nucleation in the equatorial Pacific during PEM-Tropics B: Enhanced boundary layer H_2SO_4 with no particle production. J. Geophys. Res **106**(D23), 32767–32776 (2001)

Wesely, M.L.: Parameterization of surface resistances to gaseous dry deposition in regional-scale numerical models. Atmos. Environ. **23**(6), 1293–1304 (1989)

Williams, M.B., Campuzano-Jost, P., Bauer, D., Hynes, A.J.: Kinetics and mechanistic studies of the OH-initiated oxidation of dimethylsulfide at low temperature – A reevaluation of the rate coefficient and branching ratio. Chem. Phys. Lett. **344**, 61–67 (2001)

Yvon, S.A., Saltzman, E.S., Cooper, D.J., Bates, T.S., Thompson, A.M.: Atmospheric sulfur cycling in the tropical Pacific marine boundary layer (12°S, 135°W): A comparison of field data and model results. 1. Dimethylsulfide. J. Geophys. Res. **101**(D3), 6899–6909 (1996)

Zeng, T., Wang, Y., Chance, K., Browell, E.V., Ridley, B.A., Atlas, E.L.: Widespread persistent near-surface ozone depletion at northern high latitudes in spring. Geophys. Res. Lett. **30**(24), 2298 (2003). doi:10.1029/2003GL018587

Zeng, T., Wang, Y., Chance, K., Blake, N., Blake, D., Ridley, B.: Halogen-driven low-altitude O_3 and hydrocarbon losses in spring at northern high latitudes. J. Geophys. Res. **111**(D17), D17313 (2006). doi:10.1029/2005JD006706

Zhao, C., Wang, Y., Choi, Y., Zeng, T.: Summertime impact of convective transport and lightning NO_x production over North America: modeling dependence on meteorological simulations. Atmos. Chem. Phys. **9**, 4315–4327 (2009a)

Zhao, C., Wang, Y., Zeng, T.: East China plains: a "basin" of ozone pollution. Environ. Sci. Tech. **43**, 1911–1915 (2009b)

Zhao, C., Wang, Y.: Assimilated inversion of NOx emissions over east Asia using OMI NO2 column measurements. Geophys. Res. Lett. **36**(6), L06805 (2009). doi:10.1029/2008GL037123

Zhao, C., Wang, Y., Yang, Q., Fu, R., Cunnold, D., Choi, Y.: Impact of East Asian summer monsoon on the air quality over China: view from space. J. Geophys. Res. **115**(D9), D09301 (2010). doi:10.1029/2009JD012745

Zhu, L., Nenes, A., Wine, P.H., Nicovich, J.M.: Effects of aqueous organosulfur chemistry on particulate methanesulfonate to non-sea salt sulfate ratios in the marine atmosphere. J. Geophys. Res. **111**(D5), D05316 (2006). doi:10.1029/2005JD006326